

Stabilization and calibration of x-ray wavelengths for anomalous diffraction measurements using synchrotron radiation

G. Evans

*EMBL Outstation Hamburg, c/o DESY, 22603 Hamburg, Germany
and Department of Physics, University of Warwick, Coventry CV4 7AL, United Kingdom*

R. F. Pettifer^{a)}

Department of Physics, University of Warwick, Coventry CV4 7AL, United Kingdom

(Received 2 May 1996; accepted for publication 25 July 1996)

An apparatus and technique are described for the characterization and energy stabilization of a monochromatic x-ray beam from a synchrotron radiation source that is used for diffraction experiments. The energy of the beam between 6–30 keV can be absolutely measured to an accuracy of 0.3 eV and continuous stability can be guaranteed to 0.2 eV for the duration of an experiment. The particular case of multiple wavelength anomalous diffraction is considered in detail. © 1996 American Institute of Physics. [S0034-6748(96)03710-0]

I. INTRODUCTION

Anomalous x-ray diffraction exploits the energy dependence of atomic scattering to provide additional physical information not normally present in conventional scattering. Anomalous data are obtained by choosing energies in the vicinity of an x-ray absorption edge. In order to use this technique, it is important to know the x-ray energy and its bandwidth, and to be able to maintain identical conditions for the duration of a diffraction experiment. Anomalous diffraction is widely used in two areas, scattering from amorphous material and macromolecular crystallography. It normally requires a tunable source that can be provided by synchrotron radiation. In this article we make specific reference to multiple wavelength anomalous diffraction (MAD)^{1–3} from protein crystals.

In MAD, the anomalous scattering of heavy atoms within a protein crystal is used to determine the positions of the heavy atoms and, thereafter, calculate a set of structure factor phases that together with measured diffraction amplitudes lead to an experimentally determined electron density for the protein molecule. The observed diffraction from typical protein crystals is usually much weaker than from a typical small molecule crystal, and measuring a complete set of diffracted intensities can take many hours. Coupled with the fact that the data must be measured at several wavelengths (typically three or four) a MAD experiment can easily take a day or more to perform. The unpredictability of conditions at some synchrotrons may mean that an experiment must be abandoned and continued at a later date. As such, it is important that identical beam characteristics can be reproduced over widely differing times and in some circumstances on different apparatus.

The form of the anomalous scattering near a characteristic absorption edge is largely dependent on the local environment of the scattering atom. This implies that one type of atom may display different anomalous scattering amplitudes at slightly different x-ray energies depending on its coordi-

nation geometry and ligand species. This is the so-called x-ray absorption near edge structure. It is, therefore, important to measure directly the anomalous scattering factors for a heavy atom within the protein crystal. This is typically done by measuring x-ray fluorescence from the protein crystal sample as a function of the incident x-ray energy. Frequently, the diffraction apparatus is nonoptimal for fluorescence measurements, and a specialized x-ray spectrometer can provide more accurate data. From fluorescence data it is possible, via the optical theorem⁴ and Kramers–Kronig analysis, to calculate both the real and imaginary parts of the anomalous scattering factor. Once the anomalous scattering factor spectra have been determined, selection of the appropriate x-ray energies for measuring diffraction data is possible.

Precise selection of the x-ray energy for MAD is crucial. Not only must the initial choice of x-ray energies be correct but it must be possible to select these energies on an x-ray beam line, stabilize them, and also reproduce them if the x-ray energies are to be regularly interchanged. The usual way of performing these tasks is to interpret the x-ray energy axis on which the fluorescence spectrum has been measured in terms of the angular motor step position of the monochromator. Various x-ray energies are then produced by simply driving to predetermined monochromator motor positions. This method alone, however, has several disadvantages. First, the x-ray energy axis and the monochromator motor step position are continually shifting with respect to one another because of two effects, temperature fluctuation of the monochromator crystal, and changes in the position of the synchrotron electron orbit. These difficulties have in turn been dealt with by regular recalibration of the monochromator motor step axis to a standard absorption edge (with metal foils for example). With this method, the problem will always remain, however, that the x-ray energy may still fluctuate during exposure of the protein crystal sample, as recalibration can only take place when data are not being measured. It would be desirable, therefore, to have an instrument that could provide a monochromator and source independent

^{a)}Electronic mail: pettifer@trebor.phys.warwick.ac.uk

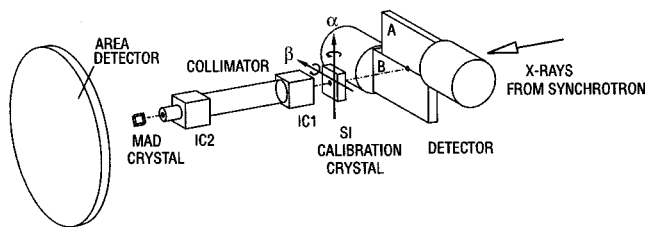


FIG. 1. Schematic diagram showing the calibration apparatus in a geometry applicable to typical diffraction experiments. X rays from the monochromator and mirror pass through the calibrator detector that consists of plastic scintillator bars A and B. Part of the beam hits the calibration crystal and at appropriate x-ray energies is diffracted back to the detector. The rest of the beam passes through the crystal and proceeds via the collimator to the crystal under study, which diffracts onto an image plate area detector.

measurement of the incident x-ray energy while also providing energy stabilization during an x-ray exposure.

In addition to x-ray energy calibration and stabilization, it is also important to measure the energy bandwidth as this affects the value of the anomalous scattering factor. This must be known in order for the results to be transferable over time and apparatuses. The instrument should also allow reproducible x-ray energy changes. Such a device has been installed on the EMBL X31 beam line on the DORIS III synchrotron in Hamburg, and is the subject of this article.

II. DESCRIPTION OF APPARATUS

The apparatus employs back diffraction of part of the x-ray beam from a perfect silicon crystal and consists of two parts, as shown in Fig. 1. A narrow band of synchrotron radiation is selected by a monochromator and focused onto the center of a rotation camera that is preceded by a collimator. In order to get to the entrance of the collimator, the beam passes unimpeded through a calibration detector and is incident onto a hole drilled into a calibration silicon crystal. Most of the radiation passes through the hole, and proceeds to the normal diffraction experiment. However, a small part impinges on the edge of the hole and if the diffraction conditions hold, a backdiffracted beam is observed by the detector of the calibration device. The silicon crystal is mounted on a goniometer that allows rotation about vertical and horizontal axes.

The detector consists of two bars of plastic scintillator (NE Technology Pilot U) mounted above and below the path of the monochromatic beam. The bars are light insulated by wrapping all but one of the small faces in thin aluminium foil. The open face of each bar is cemented to the front window of a photomultiplier tube (EMI 9814B) using optical coupling grease. The whole arrangement is contained in an aluminium housing with an aluminium foil window facing away from the synchrotron to accept backwardly diffracted x rays from the silicon crystal. The apparatus is operated in backdiffraction mode since at large Bragg angles the x-ray energy at which a diffraction line is excited is less dependent on the Bragg angle. This renders the apparatus relatively insensitive to beam movement. We define a reference orientation of the silicon crystal such that its (001) reciprocal lat-

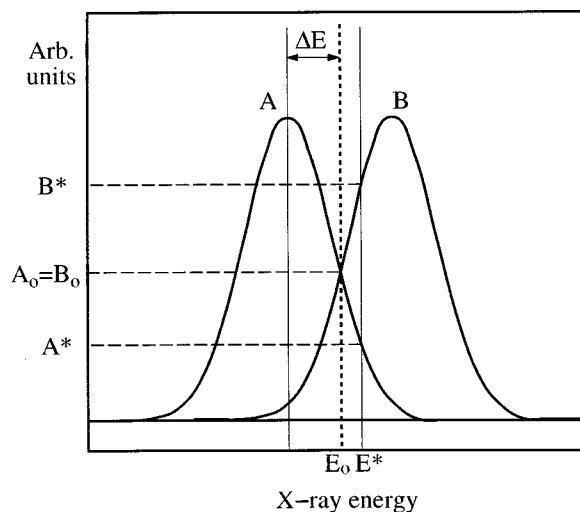


FIG. 2. Schematic diagram demonstrating the principle of x-ray energy stabilization using an hkl $h\bar{k}\bar{l}$ pair to straddle the desired energy. At the reference energy E_0 , the signals in the two calibration channels A and B are equal. A positive shift in energy, for example, to E^* effects a change in observed count rates in the calibration channels. In the case shown $B^* > A^*$ and the monochromator will be adjusted so as to lower the x-ray energy until the desired energy E_0 is achieved once again. Alternatively, if the momentary x-ray energy E^* becomes less than E_0 , the correction will be in the positive direction. The monochromator is, thus, continually adjusted so as to maintain a constant x-ray energy E_0 .

tice vector points vertically upwards and its (220) vector points back towards the detector and the source. Rotations away from the reference orientation about the vertical and horizontal axes are described by the angles α and β , respectively. In the reference orientation, the geometry is such that when x rays are incident on the silicon crystal hkl and $h\bar{k}\bar{l}$, reflections are observed in the upper (A) and lower (B) channels of the detector, respectively, at the same x-ray energy. Scanning over a range of x-ray energies with the primary monochromator produces identical results in both detector channels. Adjusting the β angle of the crystal away from $\beta=0$ has the effect of increasing the Bragg angle of say hkl reflections while decreasing the Bragg angle of $h\bar{k}\bar{l}$ reflections. This results in a splitting of hkl and $h\bar{k}\bar{l}$ pairs in energy space. A rotation of the crystal about the vertical axis (α), however, has the effect of shifting hkl $h\bar{k}\bar{l}$ pairs upwards or downwards in energy space in tandem. By adjustment of the crystal orientation, it is possible to place a pair of reflections so that they straddle any chosen x-ray energy.

The method of energy stabilization first relies on being able to position an hkl $h\bar{k}\bar{l}$ pair of reflections on either side of the desired energy, whence, the situation shown in Fig. 2. In the case shown the reflection recorded in channel A has its centroid below the reference energy at $E_0 - \Delta E$, and the reflection in channel B has its centroid above at $E_0 + \Delta E$, where ΔE is approximately half the FWHM of the calibration reflection. ΔE is, therefore, approximately equal to half the energy resolution of the beam line concerned. Any hkl $h'\bar{k}'\bar{l}'$ may also be used but setting up is most convenient for an hkl $h\bar{k}\bar{l}$ pair. At the reference energy, the falling edge of the reflection in A and the rising edge of the reflection in B intersect, implying that the signals in the A and B channels

are identical. Any change in energy away from E_0 is observed as an increase in signal in one channel and a corresponding decrease in the signal from the other. This is the basis of the stabilization technique. A software feedback loop to the monochromator axis has been employed to maintain equal signals in channels A and B.

The sensitivity of the system to x-ray energy fluctuations depends on the half-width of the reference reflections (ΔE). The half-width directly determines the rate of change of the calibrator signals as a function of x-ray energy.

Owing to the back reflection geometry, the response of the calibration apparatus to a truly monochromatic beam as a function of energy is usually much narrower than the bandwidth of the radiation from the monochromator. The conditions necessary to ensure the above are that: first, the reflections should be vertical (to minimize the effects of horizontal divergence from the mirror), i.e., $h=k$, and second, the Bragg angle should be close to 90° . Under these conditions, the width of the calibration peaks, which is the convolution of the monochromator and calibrator responses, gives a direct measure of the bandwidth of the incident radiation being used for the diffraction experiment.

A similar apparatus to that described here has been built and is in continuous operation for x-ray absorption measurements. An analysis of this instrument⁵ shows that by scanning the monochromator and observing splittings of diffraction peaks it is possible to determine α and β angles of the calibrator from which, given the known d spacing of silicon, it is possible to calculate the energy of the calibration detector peaks. If the silicon crystal lattice parameter is measured using interferometry, then the calibration can be made absolute. In our case, this is deemed unnecessary as the lattice parameter can be deduced to better than $1:10^6$ by knowing the temperature, pressure, and impurity concentration of the crystal.

III. RESULTS

The apparatus described in the previous section was set up on the anomalous diffraction protein crystallography bending magnet beam line D1/2 on Doris III. Typically, the ring operates at 4.4 GeV with a current of 100 mA in five bunch mode. Under these conditions, the calibration line peak intensities are $\sim 10^5$ counts/s with a background of $\sim 10^3$ counts/s. At these count rates, 10% changes in the relative signals from the two calibrator channels can be detected every tenth of a second. A 10% relative signal change typically corresponds to an energy sensitivity of typically 0.05 eV.

For high resolution work, a (311) silicon monochromator is employed on the beam line, although (111) crystals have also been used successfully. Step sizes of the monochromator drive limit the present stabilization to 0.22 and 0.1 eV for the (111) and (311) monochromator cases when working at a typical MAD energy of 10 keV.

A. Measuring the energy stability of a monochromatic x-ray beam

The x-ray energy stability of the beam line was determined by scanning the monochromator over a single calibra-

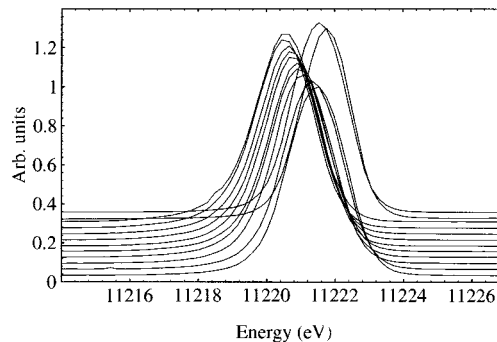


FIG. 3. Reflection profile of the calibrator's 573 reflection ($\sim 11\,220$ eV) measured at ~ 15 min intervals over one lifetime of the electron beam and at the beginning of the next electron fill. All profiles have been normalized such that the background level is zero and the peak height is unity. For clarity, successive profiles have been shifted vertically upward.

tor reflection (573) at regular time intervals over the lifetime of the electron current in the DORIS III synchrotron. The reflection profiles were then plotted as a function of the approximate x-ray energy determined from the monochromator motor position. The results are shown in Fig. 3. A total shift in x-ray energy calibration of 1.1 eV was observed over the first fill and a further 1.3 eV after the fresh injection of electrons. This illustrates the diagnosis of energy drift of the x-ray beam with monochromator temperature and/or vertical electron beam movement.

Independent measurements of maximum changes of monochromator temperature ($\Delta T = 40^\circ\text{C}$) and vertical electron beam source shift ($500\ \mu\text{m}$), can by themselves account for the observed 1.3 eV shift. The temperature change of the monochromator, caused by the 60 W heat loading, does not cause a major problem to the operation of the monochromator providing there is no differential in temperature between the diffracting surfaces. The latter effect may be observed transiently on reinjection of the electron beam.

B. Measurement of the energy resolution of an x-ray beam

The energy resolution of the X31 beam line is governed by three factors: (i) The natural width of the monochromator reflection, (ii) the vertical source size, and (iii) the vertical divergence defining slit size. In the present case, the latter was positioned just in front of the monochromator 11 m from the source. The energy resolution for a number of vertical slit settings was measured. The profile of the calibrator's 553 reflection, which is excited at ~ 9570 eV, was measured by scanning the monochromator about this energy. Gaussians were then fitted to the profiles using least squares minimization. The calculated FWHM were then plotted as a function of the slit height and shown in Fig. 4. The FWHM of the 553 reflection reaches a minimum at a slit setting of $400\ \mu\text{m}$. It is interesting to note that as the slits are closed further a broadening of the line is observed. Given an x-ray wavelength of $\sim 1.29\ \text{\AA}$ and a slit size of $50\ \mu\text{m}$, Fraunhofer diffraction theory predicts a total angular spread of $5.2\ \mu\text{rad}$ incident onto the (311) planes of the monochromator ($\theta_B = 23.2^\circ$) leading to an apparent increase of the monochromator band-

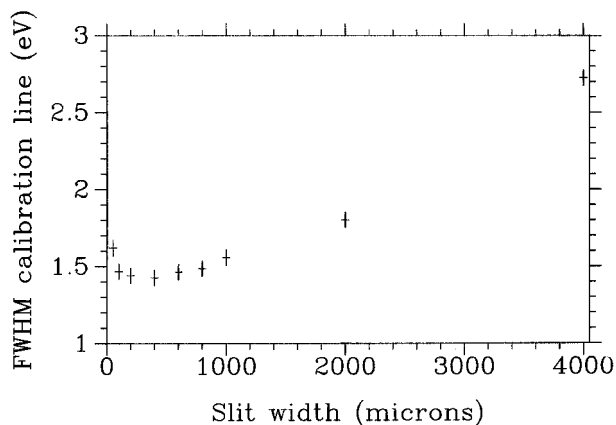


FIG. 4. Apparent energy resolution of the X31 beam line plotted against the vertical divergence defining slit height. This slit is in front of the monochromator at 11 m from the source.

pass of ~ 0.12 eV. This is compared to the observed increase in bandpass as detected by the calibrator of 0.2 ± 0.05 eV. The discrepancy between the diffraction estimate and that given by the calibrator is accommodated by the error in slit size measurement that is estimated at ± 30 μm . The slits have a high heat load, and parallelism to better than this figure cannot be guaranteed.

C. Application to a MAD experiment

To test the x-ray energy stabilization procedure, a MAD experiment was performed (the details of which will be published elsewhere⁶) on an Ir derivative crystal of hen egg-white lysozyme. X-ray fluorescence was measured from the derivative crystal across the Ir L_{III} absorption edge and transformed into the anomalous scattering factors f' and f'' using the program CHOOCH⁷ based on the method of Hoyt *et al.*⁸ The experiment was performed at five x-ray energies at and around the Ir L_{III} absorption edge. These are summarized in Table I. Data sets 3, 4, and 5 were measured using the energy stabilization procedure that provided an estimated stability of ± 0.3 eV (larger differences between the two calibration channels were tolerated during the experiment). Fluorescence spectra recorded from the protein sample over Ir L_{III} absorption edge were placed on an absolute energy scale using the technique described in Ref. 5. The protein crystal was found to contain six weakly bound iridium atoms per lysozyme molecule. Structure factor phases were calculated

using information obtained from the anomalous scattering of these iridium atoms using the program MLPHARE.⁹

In the case of MAD, where no native structure is available, the structure factor equation for the heavy atom structure in the unit cell can be written

$$F_i = \sum_{j=1}^N O_{ij}(\Delta f'_{ij} + i f''_{ij}) \exp i(\mathbf{h} \cdot \mathbf{r}_{ij}) \exp(-2B_{ij}) \quad (1)$$

$$= \sum_{j=1}^N (O'_{ij} + i O''_{ij}) \exp i(\mathbf{h} \cdot \mathbf{r}_{ij}) \exp(-2B_{ij}), \quad (2)$$

where O_{ij} is the physical occupancy of the j th heavy atom, \mathbf{r}_{ij} its positional coordinate in the unit cell, B_{ij} its temperature factor, and the subscript i represents the i th data set. Anomalous scattering factors for the j th atom, $\Delta f'_{ij}$ and f''_{ij} from Eq. (1) are combined with the occupancy O_{ij} in to yield O'_{ij} and O''_{ij} in Eq. (2). Here, $\Delta f'_{ij} = f'_{4j} - f'_{ij}$, i.e., the difference in the real part of the anomalous scattering factor between the reference data set and the i th data set.

The iridium atom parameters fitted during phase calculation were position (\mathbf{r}_{ij}), isotropic temperature factor (B_{ij}), and the real and imaginary occupancies (O'_{ij} and O''_{ij}). O'' is representative of the Friedel differences in the measured diffraction data whereas O' accounts for the dispersive anomalous differences in the data for each wavelength with respect to a reference data set that, in this case, was chosen to be data set 4 (having minimum f').

Given that the physical occupancies of the iridium sites are invariant between the five data sets, changes in O' and O'' for any one iridium atom between data sets should reflect only the anomalous scattering. We used this assumption in comparing the experimentally measured anomalous scattering factors with the fitted values of O' and O'' for one iridium atom. Since it was not possible to make an absolute estimate of the heavy atom occupancies, average occupancies were calculated using the known measured anomalous scattering factors and the refined occupancy parameters O'_i and O''_i in the following way:

$$\overline{O'} = \left(\frac{O'_i}{\Delta f'_i} \right), \quad (3)$$

$$\overline{O''} = \left(\frac{O''_i}{f''_i} \right). \quad (4)$$

TABLE I. Summary of anomalous scattering factors for iridium derivatives of lysozyme collected at five different energies around the iridium L_{III} absorption edge using the X31 beam line. Anomalous scattering factors for the five x-ray energies measured from fluorescence and processed via a Kramers–Kronig analysis compared with those calculated from the refined real and imaginary occupancies in phase calculation.

No.	Energy (eV)	Kramers–Kronig		Refined	
		f''	f'	f''	f'
1	12 300.0	8.7 ^a	−8.4 ^a	9.1	−10.3
2	11 190.0	4.1	−16.1	4.9	−15.8
3	11 214.7	19.7	−16.8	19.1	−14.8
4	11 211.5	12.1	−24.0	10.7	−24.0
5	11 217.6	13.4	−10.9	12.9	−11.7

^aValues calculated using the program CROSSEC (Ref. 11).

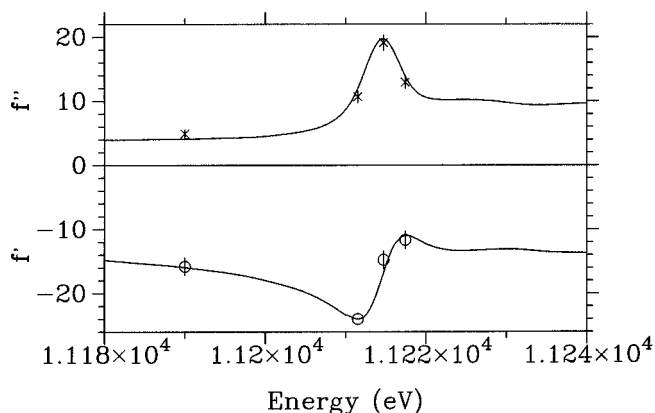


FIG. 5. Refined values of f' and f'' (electrons) for Ir in lysozyme at the L_{III} absorption edge from four data sets at different energies. The vertical lines at each data point are set at $\pm 2 \times$ standard error. The solid lines are derived from Kramers-Kronig analysis of fluorescence data.

Data set 4, being the reference set ($O'_i = 0$), was excluded from the calculation of $\overline{O'}$. We have omitted the subscript j since we are now dealing with one specific heavy atom.

The self-consistency of the data was tested by dividing the refined real and imaginary occupancies by the averages $\overline{O'}$ and $\overline{O''}$ to yield the anomalous scattering factors from refinement during phase calculation. In the case of the real anomalous scattering factors only relative values are obtained so a constant offset equal to f' for data set 4 was applied:

$$f'_i = O'_i / \overline{O'} + f'_4 \quad (5)$$

and

$$f''_i = O''_i / \overline{O''}. \quad (6)$$

f'_i and f''_i are plotted together with the experimentally measured anomalous scattering factors in Fig. 5 and are listed in Table I. The refined values agree with the curve calculated from Kramers-Kronig analysis of the fluorescence data at the 2σ level. The maximum derivative of the f'_i and f''_i curves is ~ 3 electrons/eV, illustrating the need for energy stability.

IV. DISCUSSION

The instrument function of the line can be very easily measured. For experiments where the features of the absorption edge in question are naturally broad, it may be appropriate to use a broader bandpass that will typically produce higher fluxes on the sample. In such cases, the calibrator allows the bandpass to be easily optimized for the particular experiment being performed and for the appropriate energy averaged structure factor to be obtained.

One very important aspect of the calibrator is its reproducibility when many changes of x-ray energy are performed. A typical philosophy adopted for MAD experiments is that first proposed by Hendrickson *et al.*,³ whereby systematic error in the experimental data is reduced by attempting to measure all intensities relevant to the calculation of one structure factor phase under similar conditions, i.e., pref-

erably on the same diffraction image and very close together in time in the hope that errors introduced by radiation damage to the sample crystal are minimized. This idea requires that the same region of reciprocal space in the sample crystal be recorded at all three or four x-ray energies before proceeding on to the next region. A good example of where poor energy reproducibility was apparent in a MAD experiment was given by Weis *et al.*,¹⁰ where an experiment at the Ho L_{III} was performed. The Ho L_{III} edge has a very prominent white line feature giving rise to very large rates of change of the anomalous scattering factors with x-ray energy. Indeed the nonreproducibility of energy led to changes in these scattering factors of $\sim 40\%$ in the extreme case. In this case, the structure could still be solved by performing individual refinement of the anomalous scattering factors within each region of reciprocal space. Many MAD experiments may still be unsuccessful using the latter approach because of problems with energy instability or reproducibility that cannot be diagnosed or corrected at the beam lines in question.

In addition, the apparatus has also been successfully used as a general diagnostic tool on the X31 beam line. In particular, by choosing reflections that enter the detector in the horizontal plane with relatively low Bragg angles (of say, 50° – 60°), then these conditions make the calibrator sensitive to the horizontal divergence of the beam. A horizontal intensity profile of the beam can, thus, be measured from one of these reflections. This has been found to be very useful in alignment of the toroidal mirror on the X31 line.

With the calibrator, it is now possible to essentially remove an important set of systematic errors from MAD data collection. Namely those associated with changes in the incident x-ray energy. The calibrator also opens a new possibility for minimizing systematic error in MAD experiments, whereby very accurate selection of the energy can allow data sets to be measured where the absorption coefficient of the sample crystal are the same, for example, at the rising and falling inflection points of a white line. This minimizes errors present in the data due to absorption of the scattered x rays by the sample.

A practical apparatus has been constructed and is now in routine use on the X31 beam line in Hamburg, which is dedicated to protein MAD crystallography. The instrument, however, is of general crystallographic use where ever the energy (wavelength) and or bandpass of the x-ray beam are important experimental parameters while using synchrotron radiation. The installed instrument is currently capable of maintaining stability of the x-ray energy to 0.2 eV for the duration of an experiment. The apparatus described herein has been found to be invaluable in conducting MAD experiments at Hamburg.

ACKNOWLEDGMENT

One of the authors (G.E.) thanks the European Molecular Biology Laboratory for a predoctoral fellowship.

¹J. C. Phillips, Ph.D. thesis, Stanford University, CA (1978).

²J. C. Phillips, A. Wlodawer, J. M. Goodfellow, K. Watenpaugh, L. Sieker,

- L. H. Jensen, and K. O. Hodgson, *Acta Crystallogr. Sec. A* **33**, 445 (1977).
- ³W. A. Hendrickson, J. L. Smith, and S. Sheriff, *Methods Enzymol.* **115**, 41 (1985).
- ⁴R. James, *The Optical Principles of the Diffraction of X-rays* (Bell, London, 1969).
- ⁵R. F. Pettifer and C. Hermes, *J. Appl. Crystallogr.* **18**, 404 (1985).
- ⁶G. Evans and K. S. Wilson (unpublished).
- ⁷G. Evans, Ph.D. thesis, Dept. of Physics, University of Warwick (1994).
- ⁸J. Hoyt, D. de Fontaine, and W. Warburton, *J. Appl. Crystallogr.* **17**, 344 (1984).
- ⁹Z. Otwinowsky, in *Isomorphous Replacement and Anomalous Scattering, Proceedings of the CCP4 Study Weekend, SERC/CCP4*, edited by W. Wolf, P. Evans, and A. Leslie (SERC, Daresbury Laboratory, Daresbury, 1991), pp. 80–86.
- ¹⁰W. I. Weis, R. Kahn, R. Foume, K. Drickamer, and W. A. Hendrickson, *Science* **254**, 1608 (1991).
- ¹¹D. Cromer and D. Libermann, *J. Chem. Phys.* **53**, 1891 (1970).